International Nano Letters (2019) 9:99–107
https://doi.org/10.1007/s40089-018-0263-1

ORIGINAL ARTICLE

Green synthesis of zinc oxide nanoparticles using *Solanum torvum* (L) leaf extract and evaluation of the toxicological profile of the ZnO nanoparticles–hydrogel composite in Wistar albino rats

Kenneth Maduabuchi Ezealisiji[1] · Xavier Siwe-Noundou[2] · Blessing Maduelosi[1] · Nkemakolam Nwachukwu[3] · Rui Werner Maçedo Krause[2]

Received: 10 October 2018 / Accepted: 26 December 2018 / Published online: 1 March 2019

Abstract
Current study reports a simple and one-pot synthesis of zinc oxide nanoparticles (ZnONPs) using an aqueous extract of *Solanum torvum* and evaluation of its toxicological profile (0.5% w/w and 1.0% w/w) in Wistar albino rats with respect to the biochemical index. The nanoparticles were characterized using ultraviolet–visible spectroscopy, transmission electron microscopy, Fourier transform infrared spectroscopy and X-ray diffraction technique. Dynamic light scattering (DLS) and zeta potential of synthesized nanoparticles were analyzed to know the average size and stability of particles. Synthesized nanoparticles were stable, discreet, and mostly spherical, and size of particles was within the nanometre range. Biochemical markers of hepatic and renal functions were measured. Zinc oxide nanoparticles significantly decreased serum uric acid level ($p < 0.001$) in a dose-dependent manner, while the serum alkaline phosphatase level was increased at the two test doses. The level of alanine transaminase was increased after exposure for 28 days ($p < 0.05$). This study concludes that biogenic zinc oxide nanoparticles-infused hydrogel applied dermatologically could affect hepatic and renal performance in rats, and there was an observed cumulative toxicological effect with time of exposure.

Keywords Nanoparticles · Hydrogels · Microscopy · Spectroscopy · Pharmacovigilance

Introduction

Metal oxide nanoparticles have emerged in recent years with a broad range of practical applications in electronics, photonic devices [1, 2] and biomedical field [3], including transdermal antibiotic patches and cosmetics where they are used for their sun-screening potential. Other areas include ultraviolet (UV) lasers or field emission displays [4]. Novel advances in the field of green synthesis and bio-fabrication of metal oxide nanoparticles have stimulated intense research into newer applications of zinc oxide nanoparticles in the field of nanomedicine. Zinc oxide nanoparticles have recently been well studied and used as a potential antimicrobial principle [5]. The use of zinc oxide-based nanostructures in biomedical application, especially in cosmetology either as a sun-screening or a wound-healing agent, requires their incorporation into biopolymeric matrix such as hydrogels which may be natural or synthetic. Collagen–dextran–ZnO nanoparticle composite has been reported as a wound-dressing material [6]. In their finding, 50% ZnO-infused hydrogel gave the best result for future application in wound dressing with excellent skin regeneration. However, the toxicological effect of metal oxide nanoparticles in biomedical applications such as cosmetics and wound-dressing devices needs to be properly investigated and documented. Studies have shown that nanoparticles of some metal oxides can be toxic to eukaryotic/human cells [7]. Presently, the increased toxicity of metal oxide nanoparticles due to their sub-micron-sized physical dimensions has been widely reported [8].

✉ Kenneth Maduabuchi Ezealisiji
Kenneth.ezealisiji@uniport.edu.ng

✉ Xavier Siwe-Noundou
xavsiw@gmail.com

[1] Department of Pharmaceutical and Medicinal Chemistry, Faculty of Pharmaceutical Sciences, University of Port Harcourt, Port Harcourt, Nigeria

[2] Department of Chemistry, Rhodes University, PO Box 94, Grahamstown 6140, South Africa

[3] Department of Pharmaceutics and Pharmaceutical Technology, Faculty of Pharmaceutical Sciences, University of Port Harcourt, Port Harcourt, Nigeria

Exposure to such nanoparticles is mainly through the skin and inhalation, but comparatively, copper oxide nanoparticles were reported to be more toxic than other metal oxide nanoparticles [9]. Metal oxide nanoparticles such as zinc oxide and titanium oxide are now used in several dermatological skin care products for their sun-screening effects. However, documentation on the toxicity in skin penetration enhancers such as hydrogel is not adequately reported, especially in the developing world where there is no surveillance in the area of pharmacovigilance.. Hence, present work aims at evaluating the toxicological effect of biosynthesized zinc oxide nanoparticles on biochemical markers of hepatic and renal functions.

Materials and methods

Chemicals

De-ionized Milli Q water (Merk Water Solutions), analytical-grade zinc nitrate, sodium hydroxide and other reagents used were obtained from Merck, Germany and Oxoid, Hampshire, UK.

Plant materials

Fresh leaves from the *Solanum torvum L* were collected at the Pharmacognosy garden of the University of Port Harcourt, Nigeria in March 2018. Plant sample was identified by Ekeke Chimezie of the Department of Plant Science and Biotechnology Unit of University of Port Harcourt and voucher specimen (number UP/PHCOG00056) were preserved for further use. The leaves were washed thrice with tap water followed by de-ionized water. They were further dried under shade away from direct sun light for 3 weeks, manually ground into powder and stored in an air-tight container before use.

Solanum torvum L. leaves extract preparation

The ground powdered leaves were boiled in the analytical-grade water for 45 min at 100 °C. The dark brown extract was filtered to remove insoluble fractions and macromolecules. Near ultra-filtration was then ensured using 0.45-µm sintered glass funnel and the resultant extract was stored in refrigerator at 4 °C until use. The extract obtained afforded the polyphenols and amino phyto-compounds (protein) [10] which acted as the reducing and capping agent.

Green synthesis of ZnONPs

200 ml of aqueous zinc nitrate solution (1.5 mM) was mixed with 20 ml of the aqueous leaf extract of *Solanum torvum* L. and subsequently treated with 1.0 M sodium hydroxide (10 ml). The ions which initiated the reaction were afforded by the zinc nitrate in de-ionized water. The reaction mixture was incubated with constant stirring in the dark at 60 °C to avoid photo-catalysis. An observed off-white colour marked the formation of ZnONPs at the end of 24 h. The resultant product was further purified by centrifugation and washed in double-distilled water and ethanol, respectively, dried and kept in an amber-coloured sample bottle until use.

ZnO nanoparticles–hydrogel composite preparation

2.0 kg of Ipomoea batatas (sweet potatoes) was purchased from the local market in Port Harcourt, Nigeria. Peeling, washing, wet milling and further washing with water were ensured to remove the starch. The resulting cellulosic fiber was dried in a hot air oven, pulverized and passed through a 180-µm stainless steel sieve. The product was treated with sodium hypochlorite (3.5% w/v), washed in ethanol (98% w/v) and basified to get the hydrogel. A 0.5-g quantity of ZnONPs was then infused into 95 g of the hydrogel. Both were triturated to homogeneity in a porcelain mortar and the amount made up to 100 g of the preparation with the hydrogel. Further trituration to ensure homogeneity was done. A similar step was taken to formulate the 1.0% w/w preparation

Animals

Male Wistar rats weighing 200–250 g obtained from the Animal House of the Department of Pharmacology, University of Port Harcourt, were used for the present study. They were fed with standard rodent feed (U.O.O Livestock feeds Limited, Aba, Nigeria). The rats were allowed free access to table water ad libitum. The animals were housed in an animal room maintained at 22.4 ± 1 °C and 50.6 ± 6% relative humidity with an alternating 12:12-h light–dark cycle. All animal procedures were reviewed and approved by the local institutional use of animal Ethics Committee of the University of Port Harcourt, Nigeria.

Characterization

The biosynthesized zinc oxide nano-particles were characterized by spectrophotometric and X-ray diffraction (XRD) analysis. The presence of zinc oxide nanoparticle was confirmed by UV–Vis spectroscopy (Perkin Elmer Lambda 35 UV–Vis spectrophotometer, Germany.) The UV–Vis spectral determination gives us the insight on the actual formation of the metal oxide nanoparticles by surface plasmon resonance effect. To confirm the actual phytochemical agent which was involved in capping and stabilization of ZnONPs, the Fourier transform infra-red spectroscopy (Shimadzu 8400S,

Japan) was employed. Dynamic light scattering (DLS) and zeta potential of synthesized nanoparticles were analyzed to know the average size and stability of particles (DLS-Nano2S model, UK). The crystalline nature and the average particle size were determined using XRD (Bruker: D8 Discover, Japan). Microscopic analysis was performed using scanning electron microscopy (SEM) on a TESCAN VEGA LMU, Germany as well as transmission electron microscope (TEM) on a ZEISS LIBRA 120 kV—UK, at different magnifications, to access the size, shape and dispersed nature of the nanoparticles.

Particle size analysis

The biosynthesized nanoparticles were analyzed using image processors such as Image J software. The Image J software is an image-processing entity with an inbuilt Java analytical tool. It is a Scholars domain Java-enabled programs generally used in the analysis of sub-micron images. Analysis with this processing tool affords the size distribution of particles and the average size. Other tools employed include crystallographic toolbox (CrysTBox).

Analysis of plasma zinc concentration after 7, 14 and 28 days of ZnO NPs–hydrogel composite exposure on rat skin.

Sample preparation and elemental analysis

Blood sample was centrifuged at 18,000 rpm for 20 min and blood plasma collected for use. This was treated with equal volumes of 0.5% (w/v) nitric acid in accordance with the standard method [11]. Analyses were performed against standard zinc solution prepared in glycerol (5%) to enhance the viscosity of the sample. Concentration of zinc in plasma was determined after diluting samples (1:5) with deionised water. Glycerol solution was used as a blank solution [12] during the investigation, which was conducted using atomic absorption spectrophotometer (AAS) (Perkin Elmer brand). Calibration curves for digested samples were prepared by serial dilution of stock solution in 5% glycerol. Determinations were carried out in triplicate.

Subchronic toxicity study

The rats were randomly divided into four groups of six rats each. Different doses of the bio-synthesized zinc oxide nanoparticles–hydrogel composite were applied to the rat skin to investigate the toxicity of ZnONPs on cumulative dermal exposure. A 4 cm × 4 cm area on the dorsal region of each rat was depilated once weekly. ZnONPs–hydrogel composite was applied to 10% of the total body surface area (4 cm × 4 cm). The area under drug application was covered with sterile occlusive dressing to prevent other rats from licking it up [13]. Group 1 (normal control) animals were treated with double distilled water for 28 days. Group 2 was administered dermal carbohydrate-based polymer hydrogel only as a vehicle control group [14]. Groups 3 and 4 were treated dermally with zinc oxide nanoparticles–hydrogel composite at doses of 0.5% w/w and 1.0% w/w, respectively. Previous work of Hwa Jung Ryu [15], reported that doses of 2000 mg/kg (ZnONPs only) applied repeatedly for 14 days showed significant toxicity in rats. The above report informed our consent of using a maximum dose of 1000 mg/kg in this study. A 28-day repeated-dose application was conducted for biochemical parameters [16]. This procedure was repeated every day for 28 days. At the end of 28 days, the animals were killed (euthanasia) [17] and blood sample was taken for analysis.

Result and discussion

UV–Vis spectroscopy

In the present bio-assisted synthesis protocols, the reaction mixture of aqueous leaf extract of *Solanum torvum* and zinc nitrate in solution produced an obvious color change after 24 h of incubation from yellowish brown to off-white. The observed color change confirmed the formation of ZnONPs. Observed colour change was due to the excitation of Surface Plasmon Resonance of ZnONPs. The UV–Vis spectra of biosynthesized zinc oxide nanoparticle using *Solanum torvum* showed absorption peak maxima at 359 nm and this is a characteristic signature for ZnONPs (Fig. 1) The shape of synthesized nanoparticles is believed to be spherical in line with Mei's theory which states that: The shape of the synthesized nanoparticle is spherical if a single sharp absorbance peak was observed in the UV–Vis spectrum [18].

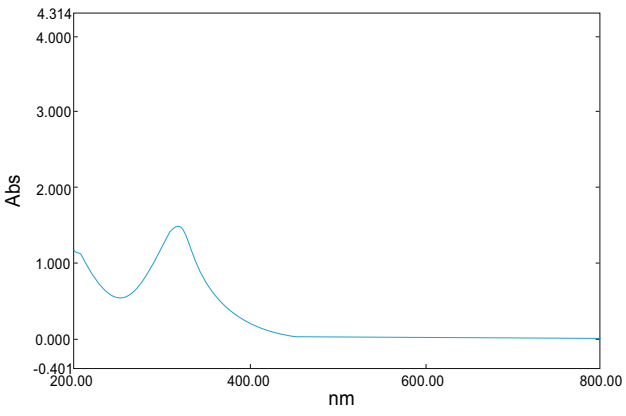

Fig. 1 UV–Vis spectroscopic analysis of synthesized zinc oxide NPs, a single peak corresponding to zinc oxide nanoparticles (359 nm)

Proposed mechanism of synthesis of ZnONPs through *Solanum torvum*

In the green synthesis of ZnONPs, the possible phytochemical agent that can reduce Zn^{2+} to ZnO, and hence aggregates of ZnO nanoparticles are polyphenols (Quercetin). The richly available alkaloids and flavonoids in the plant extract acted as stabilizing and capping agents, respectively. These phytochemicals were revealed in the FTIR signature. Hence, the proposed principle of formation of ZnONPs involves the ionization of zinc nitrate in an aqueous medium to give Zn^{2+} which was reduced by phytochemical principle present in the aqueous extract of *Solanum torvum*, especially quercetin (a polyphenol), to generate ZnO, which further aggregates to ZnONPs as shown below (Fig. 2).

FT-IR analysis

Biosynthesized zinc oxide nanoparticles in *Solanum torvum* aqueous extract was analyzed using FT-IR (Bruker, Germany) within the scan range of 4000–5000 cm^{-1} to ascertain the possible phytochemical principle which is implicated in capping and stabilization. The spectral data study shows that synthesized nanoparticles exhibit (broad, sharp) peaks at 3362 cm^{-1} corresponding to O–H bond of phenols and 1620–1652 cm^{-1} corresponding to C=O stretching vibration of primary amines. There are also the prominent amide I and II vibrations at 1389 cm^{-1} and 1068 cm^{-1} (Fig. 6). The above inference justifies the fact that the presence of phenols, polyphenols and primary amines in the plant extract could be implicated for capping and stabilization of ZnONPs. Our findings are in agreement with the previous work obtained from zinc oxide nanoparticles synthesized from *Catharanthus roseus* (L) leaf extract [19]. Justification of formation of metal and metal oxide nanoparticles in phytochemically assisted synthesis strictly requires clear FTIR information, showing that phytochemicals present in the plant extract actually assisted in such synthesis. It is very important in any of such synthesis to pin-point the functional group present in the extract, which has really taken part in such synthesis. Present FTIR studies aim to reveal the functional groups and, hence, chemical entity that was involved in the green synthesis of ZnONPs (capping and stabilizing agents). The FTIR studies of the synthesized ZnONPs and the ZnONPs–hydrogel composite are shown below (Fig. 6) There was no apparent change in the spectral pattern showing that the nanoparticles were actually stabilized and capped by the phytochemical agents and the integrity of the nanoparticles was maintained in the hydrogel.

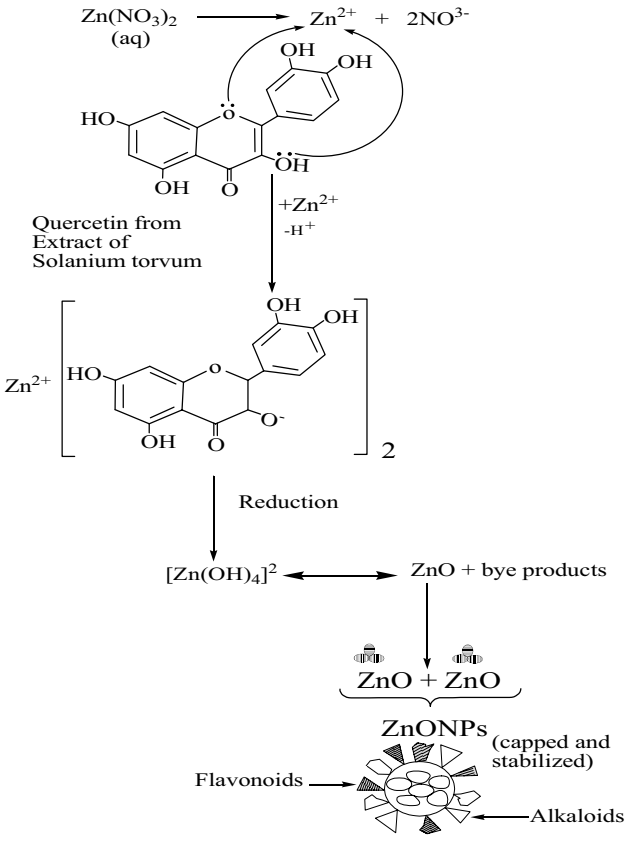

Fig. 2 Proposed mechanism of synthesis of ZnONPs through *Solanum torvum*

XRD analysis

The X-ray diffraction (XRD) pattern of the biosynthesized sample of Zinc Oxide nanoparticles was recorded at the Department of Chemistry, Rhodes University Nanotechnology Centre using Bruker d8 Advanced X-ray diffractometer, using CuKα radiation ($\lambda = 1.5406$ Ä) 40 kV, 2 Θ/Θ scanning mode. Data were obtained for the 2Θ range of 10°–100° in a step proceeding of 0.0204 degree. The diffractogram (Fig. 3) presented with six peaks at 2Θ values of 18.203°, 20.937°, 23.671°, 30.108°, 34.608°, and 40.204° corresponding to (020), (022), (022), (111), (120), and (200) integer on

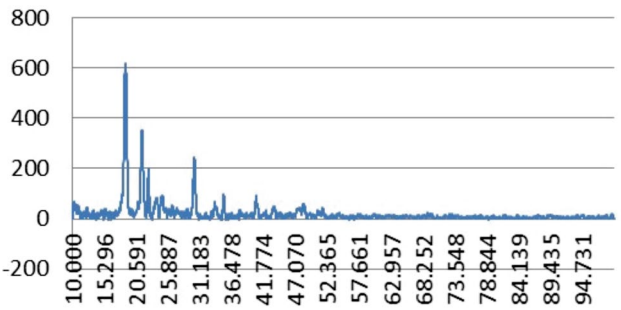

Fig. 3 XRD analysis of synthesized ZnO NPs which captured eight Bragg reflections corresponding to the spherical crystalline nature of the nanoparticles

the 'hkl' planes, respectively. This indicates spherical but discreet crystalline nature of the particulate matter with few end-centered monoclinic crystalline shapes. This result was in correlation with marched data from International Centre for Diffraction Data (ICDD). Optimum Bragg reflection was obtained at 2Θ of 18.402° to predict full width half maximum (FWHM) value as the average size of the zinc oxide nanoparticle was calculated to be 28.24 nm using the following Debye–Scherrer equation:

$$D = \frac{K\lambda}{\beta \mathrm{Cos}\theta},$$

where D is the thickness of the nanocrystal, K is a constant; λ is the Bragg`s angle 2Θ.This result was strongly supported by the one obtained from DLS–Zeta sizer which gave 28.21 ± 6.369 average particle size. Unassigned crystalline peaks (42.8°, 48.2° and 51°) are also recorded in the XRD pattern which is attributed to the presence of crystallized phytochemicals on the surface of the zinc oxide nanoparticles (Capping and stabilizing agents).

TEM and SEM analysis

The high-resolution studies with TEM analysis revealed that the particles were discreet, spherical in nature and polydispersed (Fig. 4a) with size ranging from 34 to 40 nm and mean particle size of 38.0 ± 2 nm. Studies of SEM micrograph reveal a non-smooth, but spherical morphology of the nanoparticles with a few monoclinic non-spherical particles (Fig. 4b).

DLS and zeta potential

The size distribution image (DLS) of biosynthesized zinc oxide nanoparticle is represented in Fig. 5. Observation shows that the size distribution of zinc oxide nanoparticles ranges from 15 to 45 nm. The calculated average particle size distribution of this nanoparticle is 28.21 ± 6.369. The multifunctional application of DLS analyzer confirms the result of the particle size of synthesized zinc oxide nanoparticles obtained in earlier report from XRD (28.24 nm). The zeta potential of the biosynthesized zinc oxide nanoparticle was found to be a distinct peak at 2.61 mV which suggests that the synthesized nanoparticles are positively charged and

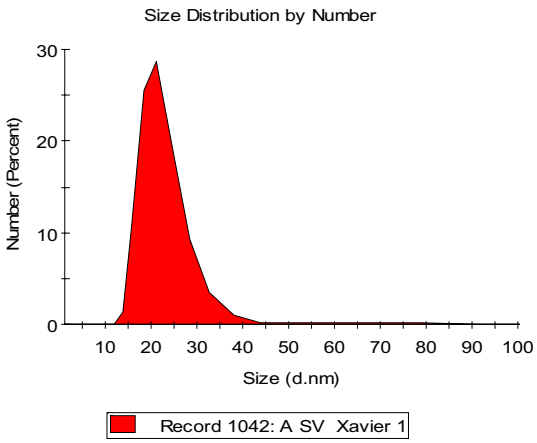

Fig. 5 DLS particle size distribution of synthesized ZnONPs

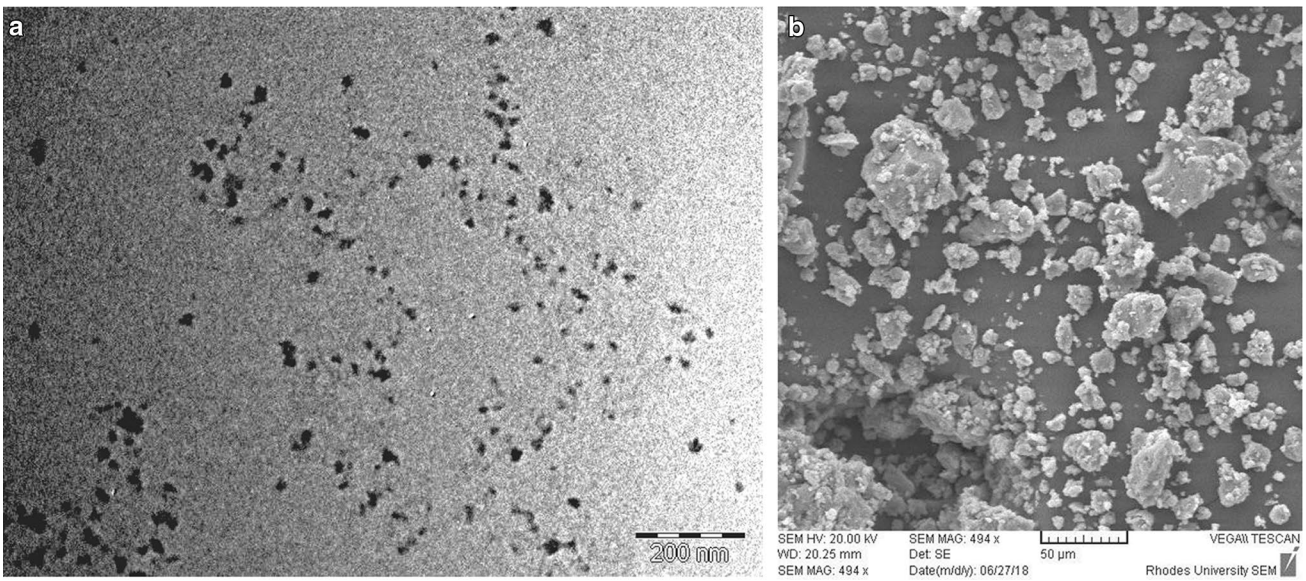

Fig. 4 **a** TEM image and **b** SEM image of biosynthesized ZnONPs

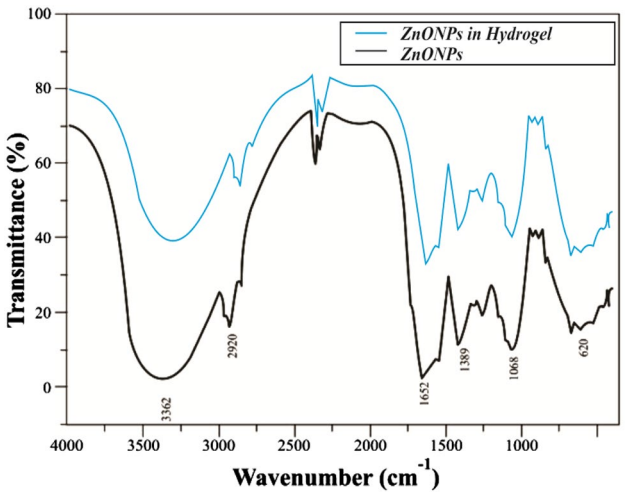

Fig. 6 FT-IR of ZnONPs in hydrogel and ZnONPs

Table 1 Plasma level of zinc at different doses of zinc oxide nanoparticles-infused hydrogel in rats

Dose	Zinc PPM		
	7 Days	14 Days	28 Days
Control	0.30 ± 0.002	0.30 ± 0.001	0.30 ± 0.004
Veh. Cont.	0.40 ± 0.001	0.30 ± 0.001	0.30 ± 0.002
0.5% w/w	1.62 ± 0.002*	1.86 ± 0.002*	1.94 ± 0.004*
1.0% w/w	2.84 ± 0.004*	3.68 ± 0.002*	5.20 ± 0.004*

Data expressed as mean ± SEM

Veh. Cont vehicle control

*Significant at $P < 0.05$

moderately dispersed in the medium, though negative values are implicated for nanoparticle stability (Fig. 6).

Plasma concentration of zinc

The plasma zinc level in all rats treated with 0.5% w/w and 1.0% w/w zinc oxide nanoparticles-infused hydrogel for 7, 14 and 28 days increased significantly in dose- and time-dependent manner, $P < 0.05$, as compared to rats in the control group (Table 1). Possibly, hydrogel being an ideal permeation enhancer, has increased skin permeability by reversibly disrupting the stratum corneum structure, hence providing an added driving force for transport of nanomaterials into the skin and blood, respectively. This was achieved through the moisturizing and humectants property of the hydrogel. Metal nanoparticles may induce oxidative stress, mitochondrial damage, DNA denaturation and hasten apoptosis of skin structure [20].

Sub-acute toxicity studies

Biochemical parameters

Serum levels of aspartate transaminase were significantly, $P < 0.05$, increased in rats that received 1% w/w zinc oxide nanoparticles-infused hydrogel for 7, 14 and 28 days; while serum levels of aspartate transaminase in all rats that were exposed to 0.5% w/w zinc oxide-infused hydrogel were not significantly different from control rats(Table 2). The serum level of alanine transaminase (AST) in rats that received 1% w/w zinc oxide nanoparticles-infused hydrogel for 14 and 28 days were significantly, $P < 0.05$, increased; while there was no significant change in ALT levels in all other treated rats when compared to control rats.

Furthermore, serum alkaline phosphatase (ALP) levels in all rats exposed to 1% w/w and 0.5% w/w zinc oxide nanoparticles-infused hydrogel were not significantly increased as compared to the serum alkaline phosphatase (ALP) levels in rats in the control group. The serum uric acid level in all rats treated with 0.5% w/w and 1.0% w/w zinc oxide nanoparticles-infused hydrogel for 7, 14 and 28 days, decreased significantly in dose- and time-dependent manner, $P < 0.01$, as compared to rats in the control group (Table 3).

The total protein level in rats exposed to zinc oxide nanoparticles-infused hydrogel did not show any significant change when compared to their corresponding level obtained in the control group (Table 4). The total

Table 2 Serum levels of transaminase enzyme at different doses of zinc oxide nanoparticles-infused hydrogel in rats

Dose	AST (IU/l)			ALT (IU/l)		
	7 Days	14 Days	28 Days	7 Days	14 Days	28 Days
Control	97.00 ± 3.08	98.00 ± 2.06	103.00 ± 2.01	26.00 ± 0.005	26.00 ± 0.005	26.00 ± 0.005
Veh. Cont	98.00 ± 2.06	97.00 ± 2.04	98.00 ± 3.02	26.00 ± 0.004	26.00 ± 0.004	26.00 ± 0.004
0.5% w/w	106.00 ± 2.01	101.00 ± 3.02	108.00 ± 2.04	29.00 ± 0.05	33.00 ± 0.05	34.00 ± 0.08
1.0% w/w	141.00 ± 2.04*	142.00 ± 2.00*	158.00 ± 0.08*	30.00 ± 0.02	36.00 ± 0.18*	38.00 ± 0.08*

Data expressed as mean ± SEM

AST aspartate transaminase, *ALT* alanine transaminase

*Significant at $P < 0.05$

cholesterol level in rats treated with 1.0% w/w Zinc oxide nanoparticles-infused hydrogel showed significant increase, $P < 0.01$, for 14 and 28 days, while the total cholesterol level in rats exposed to 0.5% w/w zinc oxide nanoparticles-infused hydrogel as well as those that received 1.0% w/w zinc oxide nanoparticles-infused hydrogel for 7 days were not significantly different from the control rats (Table 4). As compared to the control group, it can be observed that serum creatinine level increased, $P < 0.001$, in rats that received 1.0% w/w zinc oxide nanoparticles-infused hydrogel for 7, 14 and 28 days when compared to control rats; while serum creatinine levels in all rats treated with 0.5% w/w zinc oxide nanoparticles-infused hydrogel were not significantly different from control (Table 5). For serum urea levels, there were no significant changes in rats treated with 0.5% w/w zinc oxide nanoparticles-infused hydrogel as compared to the control but, it was significant, $P < 0.01$, and time dependently decreased in rats treated with 1% w/w zinc oxide nanoparticles-infused hydrogel as compared to the control rats (Table 5).

Nanoparticles have the ability to enter, translocate within and damage living tissues and organs due to their small size, which allows them to penetrate physiological barriers and travel within the circulatory systems of the host. Some nanoparticles, depending on their composition and size, can produce irreversible damage to cells by oxidative stress or/and organelle injury [21–24]. Zinc oxide nanoparticles exhibit higher toxic effects than other metallic nanoparticles and this is likely because of their ion-shedding ability. The blood biochemical tests are frequently used in assessing the functions of the kidney and liver and also to measure the response to the exogenous toxic exposure. Serum phosphatase and transaminase levels are generally used in toxicological studies to evaluate hepatic function. Elevation in the serum levels of alanine transaminase (ALT) and aspartate transaminase (AST) by the zinc oxide nanoparticles in this study indicates

Table 3 Serum levels of alkaline phosphatase and uric acid following different doses and time of exposure of zinc oxide nanoparticles-infused hydrogel in rats

Dose	ALP (IU/l)			Uric acid (µmol/l)		
	7 Days	14 Days	28 Days	7 Days	14 Days	28 Days
Control	48.00 ± 0.08	48.00 ± 0.08	48.00 ± 0.05	620.00 ± 0.08	620.00 ± 5.08	620.00 ± 5.08
V. Cont	48.00 ± 0.06	48.00 ± 0.07	48.00 ± 0.08	620.00 ± 0.06	620.00 ± 5.08	620.00 ± 5.08
0.5% w/w	50.00 ± 0.04	54.00 ± 0.02	58.00 ± 0.08	552.00 ± 3.08*	560.00 ± 5.04**	580.00 ± 6.08**
1.0% w/w	60.00 ± 0.04	62.00 ± 0.01	64.00 ± 0.01	420.00 ± 3.09*	460.00 ± 8.02**	308.00 ± 7.00**

Data presented as mean ± SEM

*Significant at $P < 0.05$

**Significant at $P < 0.01$

Table 4 Serum levels of total protein and cholesterol at different doses of zinc oxide nanoparticles-infused hydrogel in rats

Dose	Total protein (g/l)			Total cholesterol (µmol/l)		
	7 Days	14 Days	28 Days	7 Days	14 Days	28 Days
Control	82.00 ± 0.01	84.00 ± 0.01	84.00 ± 0.01	2.40 ± 0.01	2.40 ± 0.02	2.40 ± 0.04
V. Cont	84.00 ± 0.01	84.00 ± 0.01	84.00 ± 0.01	2.40 ± 0.01	2.40 ± 0.01	2.40 ± 0.01
0.5% w/w	84.00 ± 0.06	84.00 ± 0.02	80.00 ± 0.02	2.50 ± 0.01	2.50 ± 0.01	3.00 ± 0.20
1% w/w	72.00 ± 0.01	74.00 ± 0.06	76.00 ± 0.05	4.00 ± 0.01	4.50 ± 0.02*	4.80 ± 0.05*

Data presented as mean ± SEM

*Significant at $P < 0.01$

Table 5 Serum levels of creatinine and urea at different doses of zinc oxide nanoparticles-infused hydrogel in rats

Dose	Creatinine (µmol/l)			Urea (mmol/l)		
	7 Days	14 Days	28 Days	7 Days	14 Days	28 Days
Control	174.00 ± 8.04	174.00 ± 8.04	174.00 ± 8.04	7.60 ± 0.06	7.60 ± 0.06	7.60 ± 0.06
V. Cont	174.00 ± 8.04	174.00 ± 8.04	174.00 ± 8.04	7.60 ± 0.06	7.60 ± 0.06	7.60 ± 0.06
0.5% w/w	176.00 ± 3.08	184.00 ± 4.08	196.00 ± 4.02	5.20 ± 0.02	5.40 ± 0.06	5.70 ± 0.04
1.0% w/w	212.00 ± 6.03**	227.00 ± 6.04**	240.00 ± 8.01**	3.80 ± 0.06*	4.00 ± 0.01*	4.20 ± 0.02*

Data was expressed as mean ± SEM

*Significant at $P < 0.01$

**Significant at $P < 0.001$

cellular injury to the liver. Alanine phosphatase (ALP) was also increased dose and time dependently, although not significantly. This increase in the serum level of the liver enzymes indicates loss of liver cells and increased leakage of the enzyme from damaged hepatocytes. The serum uric acid measurement helps to determine how well the body produces and removes uric acid. Uric acid is usually dissolved in the blood, filtered through the kidneys and expelled in the urine. From the study, it can be deduced that the serum uric acid level decreased in a time- and dose-dependent manner indicating that repeated exposure to the zinc oxide nanoparticles could lead to oxidative stress, since uric acid is an anti-oxidant. The total protein decreased, though not in a significant manner, due to the impairment of production of albumin or globulin due to the severe liver damage and this consequently resulted in the decrease of serum levels of urea since urea is the principal nitrogenous end-product of protein and amino acid catabolism. It can also be deduced that exposure to zinc oxide nanoparticles leads to increase in total cholesterol, though not in a significant manner. This is due to the damage of the liver cell responsible for producing and clearing the cholesterol in the body and this may present some cardiovascular abnormalities with time. Creatinine is a chemical waste generated from muscle metabolism. It is transported through the blood stream to the kidneys which filter out most of the creatinine which is excreted with the urine. Thus, an elevated creatinine level as seen in the result indicates impaired kidney function due to exposure to the zinc oxide nanoparticles. Metal nanoparticles are known to inhibit cell activity by epigenetic mimicking [25–28].

Conclusion

A simple but green synthesis has been adapted for the phytochemical-assisted fabrication of ZnONPs employing aqueous leaf extracts of *Solanum torvum* L. Organoleptic confirmation justifies the color change followed by UV–Vis spectral characterization, SEM and TEM microscopy highlights the morphology of the synthesized nanoparticles as a none-smooth spherical, discreet entity with a size range of 28.0 nm. The XRD result also justified the crystalline nature and particulate size in the nano-range. There is an observed significant increase in the plasma zinc level in a dose- and time-dependent manner. Toxicological studies herein showed that biochemical markers for both renal and hepatic functions were affected by dermatological exposure of ZnO nanoparticles–hydrogel composite and could cause damage to the organs following a long period of application.

Acknowledgements The authors wish to acknowledge the Department of Chemistry, Rhodes University, GrayhamsTown, South Africa for their technical assistance.

Compliance with ethical standards

Conflict of interest The authors declare no conflict of interest.

References

1. Engelbert, R., Peter, M., Chen, H., Srebri, P., Geoffrey, A.O.: Nanoparticle films and photonic crystal multilayers from colloidally stable size-controllable zinc and iron oxide nanoparticles. ACS Nano **5**(4), 2861–2869 (2011)
2. Zbigniew, S., Mieczyslaw, B., Katarzyna, D., Grzegorz, C.: Synthesis and characterization of iron oxide magnetic nanoparticles. Nukleonika **62**, 73–77 (2017)
3. Ramos, A.P., Marcus, A.E.C., Camila, B.T., Pietro, C.: Biomedical application of nanotechnology. Biophys. Rev **9**(2), 79–89 (2017)
4. Threes, G.S., Stanislav, P.: Titanium dioxide and Zinc Oxide nanoparticles in sunscreens: focus on their safety and effectiveness. Nanotechnol. Sci. Appl. **4**, 95–112 (2011)
5. Justin, T.S., Thomas, J.W.: Antimicrobial applications of nanotechnology: methods and literature. Int. J. Nanomed. **7**, 2767–2781 (2012)
6. Mie, G.: A contribution to the optics of turbid media especially colloidal metallic suspensions. Ann. Phys. **25**, 377–445 (1908)
7. Kungang, L., Ying, C., Wen, Z., Zhichao, P., Lin, J., Yongshen, C.: Surface interactions affect the toxicity of engineered metal oxide nanoparticles towards paramecium. Chem. Res. Toxicol. **25**(8), 1675–1681 (2012)
8. Ibrahim, K., Khalid, S., Idrees, K.: Nanoparticles: properties, applications and toxicities. Arab. J. Chem. (2017). https://doi.org/10.1016/j.arabjc.2017.05.011
9. Hanna, L., Pontus, C., Johanna, G., Lennart, M.: Copper oxide nanoparticles are highly toxic: a comparison between metal oxide nanoparticle, and carbon nanotubes. Chem. Res. Toxicol. **9**, 1726–1732 (2008)
10. Raja, N.H., Lingarajau, K., Manjunath, K., Kumar, D., Nagaraju, G., Suresh, D., Nagabhushana, H.: Green synthesis of CuO nanoparticles using *Gloriosa superb* L. extract and their antimicrobial activity. J. Taibah Univ. Sci. **9**(1), 7–12 (2015)
11. Nabil, R.B.: Sample preparation for flame atomic absorption spectroscopy: an overview. Rasayan J. Chem. **4**(1), 49–55 (2011)
12. Mirela, G., Eduardo, S.C., Daiane, P.C.Q., Edmar, P.M., Adilson, J.C., Aldalea, L.B.M.: Simple method for the determination of Cu and FE by electrothermal atomic absorption spectrometry in biodisiel treated with tetramethyl ammonium hydroxide. Microchem. J. **98**(1), 62–65 (2011)
13. Lisa, A.D.: Application of nanotechnology in dermatology. J Invest. Dermatol. **132**(3), 964–975 (2012)
14. John, P.S., Kathleen, A.S., Lloyd, E.K., Prath, C.H.: Skin diseases in laboratory mice: approaches to drug target identification and efficacy screening. Methods Mol. Biol. **1438**(1), 199–224 (2016)
15. Hwa, J.R., Mu, Y.S., Sung, K.J., Eun, H.M., Seung, Y.L., Dong, H.J., Taek, J.L., Ki, Y.J., Kyu, B.C., Meyoung, K.K., Beom, J.L., Sang, W.S.: Zinc Oxide nanoparticles: a 90-day repeated-dose

dermal toxicity Study in rats. Int. J. Nanomed. **9**(2), 137–144 (2014)
16. Parasuraman, S.: Toxicological screening. J Pharmacol. Pharmacother. **2**(2), 74–79 (2011)
17. Magur, P., Najan, A.K., Kamal, K.M.: Evaluation of acute and subacute oral toxicity induced by ethanolic extract of *Marsdnia tenacissima* leaves in experimental rats. Sci. Pharm. **85**(3), 29 (2017)
18. Elias, S., Elham, G., Kazem, N.: Size-controlled and optical properties of monodispersed silver nanoparticles synthesized by the radiolytic reduction method. Int. J. Mol. Sci. **14**(4), 7880–7896 (2013)
19. Bhumi, G., Savithramma, N.: Biological synthesis of zinc oxide nanoparticles from *Catharanthus roseus* (I) G Don leaf extract and Validation for antimicrobial activity. Int. J. Drug Dev. Res. **12**(3), 2762–2779 (2014)
20. Wilhelmi, V., Fisher, U., Weighardt, H., Schulze-Osthoff, K., Nickel, C., Stahimecke, B.: Zinc oxide nanoparticles induced necrosis and apoptosis in macrophages in a p47 phox-and Nrf2-independent manner. PLoS One **8**(6), e65704 (2013). https://doi.org/10.1371/journal.pone.0065704
21. Rong, W., Yigun, M., Lingfang, F., Sufan, C., David, J.T., Qunwei, Z.: DNA damage caused by metal nanoparticles: the involvement of oxidative stress and activation of ATM. Chem. Res. Toxicol **25**(7), 1402–1411 (2012)
22. Bhadra, M.P., Sreedhar, B., Patra, C.R.: Potential theranostics application of bio-synthesized silver nanoparticles (4-in-1 system). Theranostics **4**, 316–335 (2014)
23. Baik, N.S., Sakai, G., Miura, N., Yamazoe, N.: Preparation of stabilized nanosized tin oxide particles by hydrothermal treatment. J. Am. Ceram. Soc. **83**, 2983–2987 (2000)
24. Gade, A., Bonde, P., Ingle, A., Marcato, P., Duran, N., Rai, M.: Exploitation of *Aspergillus niger* for synthesis of silver nanoparticles. J. Biobased Mater. Bioenergy **2**, 243–247 (2008)
25. Guanalan, S., Sivaraj, R., Venekatesh, R.: Aloe barbadensis Miller mediated green synthesis of mono-dispersed copper oxide nanoparticles. Optical properties. Spectrochim. Acta. A **97**, 1140–1144 (2012)
26. Hidron, A.I., Kempker, R., Moanna, A., Rimland, D.: Methicillin-resistant *Staphylococcus aureus* in HIV-infected patients. Infect. Drug Resist. **3**, 73–86 (2010)
27. Li, Y., Leung, P., Yao, L., Song, Q., Newton, E.: Antimicrobial effect of surgical masks coated with nanoparticles. J. Hosp. Infect. **62**, 58–63 (2006)
28. Vanaja, M., Annadurai, G.: *Coleus aromaticus* leaf extract mediated synthesis of Silver nanoparticles and its bactericidal activity. Appl. Nanosci. **3**, 217–223 (2012)